ISSN: 2710-0588

Study on the Differences in Mechanical Properties and Energy Evolution of Sandstone under Different Loading and Unloading Modes

Qiyu Zhang*

School of Civil Engineering, Henan Polytechnic University, Jiaozuo 454003, Henan, China

* Corresponding Author

Abstract

To study the mechanical properties and energy evolution of sandstone under cyclic loading, experiments were conducted on intact prefabricated sandstone specimens using different loading and unloading methods, and the macroscopic failure characteristics of the rock samples were observed and analyzed. The mechanical properties and energy evolution of the rock samples were analyzed based on the stress-strain curves. The results indicate that the hysteresis loop areas differ under the two loading and unloading methods. The method with increasing upper limits mainly shows that the higher the stress peak, the stronger the material's energy dissipation capacity, and the more energy is consumed by plastic deformation and damage. In the method of increasing the upper limit and decreasing the lower limit, the hysteresis loop area gradually increases, indicating that an elevated stress level enhances the material's energy dissipation capacity, and damage induces internal friction or microcrack propagation. In both loading methods, energy evolution and damage failure characteristics are dominated by the stress application pattern: the stress concentration effect in the upper-limit-increasing method accelerates the compaction of the elastic framework and energy dissipation due to damage, resulting in a greater increase in total input energy, elastic energy, and dissipated energy, and the energy conversion efficiency is also higher due to more favorable elastic energy storage. In the upper-limit-increasing and lower-limit-decreasing method, simultaneously adjusting the stress upper and lower limits weakens stress concentration, resulting in smoother energy growth and increased damage energy consumption due to stress fluctuations. The growth rate of dissipated energy density shows a 'burst-decline-leveling-off' trend, corresponding to three damage stages, revealing the non-uniform evolution of damage. The upper-limit-increasing method results in tensile failure dominated by a single vertical main crack, with damage occurring as a directional superposition effect, while the upper-limit-increasing and lower-limit-decreasing method results in dispersed failure driven by a multi-directional crack network, with damage extending at multiple scales.

Keywords

Cycle loading and unloading; mechanical properties; energy evolution; failure characteristics.

1. Introduction

In underground engineering fields such as mineral resource exploitation, transportation tunnel construction, and water conservancy and hydropower projects, rock masses are often subjected to cyclic loading (e.g., blasting vibration, mining disturbance, vehicle vibration, etc.). Compared with monotonic loading, cyclic loading induces continuous crack initiation, propagation and coalescence within rock masses, which further leads to the deterioration of

ISSN: 2710-0588

mechanical parameters and accumulation of damage, ultimately triggering the instability and failure of surrounding rock. As a widely distributed sedimentary rock in southwest China, white sandstone is extensively used as tunnel lining, subgrade filler and building stone due to its excellent engineering properties. However, the evolution law of its long-term mechanical properties under cyclic loading has not been clearly elucidated. Therefore, it is necessary to conduct in-depth research on the mechanical characteristics and energy evolution of white sandstone under cyclic loading.

Numerous scholars have conducted extensive research on the mechanical properties and energy evolution of white sandstone. Lin Zhinan [1] investigated the permeability characteristics of sandstone under cyclic loading-unloading at different temperatures. The results showed that at lower temperatures (50, 75 ℃), the compaction degree of pores and microcracks is relatively high, resulting in fewer new cracks; at higher temperatures (90 ℃), the number of cracks increases, with obvious coalesced cracks. Zhu Mingliu [2] carried out uniaxial compression and cyclic loading-unloading tests on the main lithologies of surrounding rock in coal seam roadways (sandstone, mudstone, and coal seam). Through systematic analysis of the mechanical properties and energy evolution law of surrounding rock, a rock stability evaluation method was established from an energy perspective. Zhiwei Ni [3] studied the mechanical properties and deformation-failure characteristics of sandstone under gradient constant-amplitude cyclic loading-unloading. The research results clarified the deformation and failure mechanisms of sandstone under gradient constant-amplitude cyclic loading, providing valuable insights for the stability assessment and disaster mitigation of open-pit mine slopes. Liu Yiming [4] researched the acoustic-thermal response characteristics and precursor laws of fractured sandstone under cyclic loading-unloading, analyzed the acoustic-thermal response characteristics during crack propagation, revealed the precursor laws of various acoustic and thermal signals, and proposed the coefficient of variation index for acoustic-thermal crack evolution. Huimin Yang [5] studied the evolution of characteristic parameters and damage mechanisms of sandstone under the synergistic effect of freeze-thaw (F-T) and stepped cyclic loading-unloading through real-time CT scanning and AE monitoring. The analysis showed that under the same F-T conditions, pre-cracked sandstone exhibits higher parameter changes than intact sandstone. Z. Y. Song [6] investigated the mechanical response of sandstone under triaxial differential cyclic loading with different confining stress unloading rates. The test results indicated that the strength of rock specimens under different stress paths of triaxial unloading confining stress-differential cyclic loading can be fitted using the Mohr-Coulomb, Hoek-Brown, and Bieniawski criteria. The confining stress unloading rate can dominate the radial strain rate, while the axial DCL pattern has an insignificant effect. Zhang Qihang [7] studied the energy evolution law of sandstone under different cyclic loading-unloading modes in true triaxial tests, and found that the failure strength and peak-valley strain of the maximum principal stress of rock samples under different paths all show obvious path-dependent characteristics. Zhu Ningqiang [8] researched the deformation-failure and acoustic emission response characteristics of fractured sandstone under cyclic loading-unloading, and revealed the strengthening and deterioration mechanisms of cyclic loading on the mechanical properties of fractured sandstone from the perspective of macro-mesoscopic structural changes. Hao Jianping [9] studied the damage mechanical properties and energy evolution of hard rock under cyclic loading-unloading with different upper limit stresses, and found that the damage degree of sandstone presents a linear relationship with the number of cycles. Cheng Jianchao [10] investigated the post-peak mechanical mutation behavior of sandstone under triaxial cyclic loading-unloading, indicating that the design of triaxial cyclic loading-unloading tests can provide a reliable method for hierarchically revealing the post-peak mechanical mutation behavior of sandstone. Tang Jinzhou [11] studied the mechanical response characteristics and seepage evolution law of sandstone with inclined single fractures under

ISSN: 2710-0588

cyclic loading. It was revealed that the protrusions on the fracture surface are worn and sheared during sliding; the shearing and wear of protrusions lead to slight stress drops during loading, which is also the main reason for the fluctuation of flow rate during compression. Xiao Fukun [12] researched the damage characteristics of rock under multi-level characteristic stress cyclic loading-unloading, and elaborated on the damage characteristics of fine sandstone at different stress stages from the perspectives of energy consumption and damage quantity. Wang Mengxiang [13] conducted an experiment on the energy dissipation of blast-damaged roof sandstone under triaxial graded cyclic loading-unloading. The results showed that blast loading damage changes the internal structure of the rock mass, making the energy consumption ratio of the specimens more significant under cyclic loading-unloading. Cheng Jianchao [14] analyzed the deformation characteristics and established a dilatancy percolation model of sandstone under triaxial cyclic loading-unloading. It was revealed that the brittle deformation and failure of sandstone are inhibited under the action of water, and the theoretical prediction of the established percolation model is highly consistent with the measured data during the crack propagation stage. Liu Guangjian [15] studied the macro-mesoscopic damage characteristics of fractured sandstone under cyclic loading-unloading with variable upper limits. The results provide a reference for the scientific evaluation of engineering stability. Jia Peng [16] carried out tests on the resistivity and acoustic emission response of red sandstone under cyclic loading-unloading, revealing that the change in resistivity is in good consistency with stress. Zhao Guozhen [17] studied the failure mechanical behavior and energy evolution law of coal-rock mass based on cyclic loading-unloading. The research results showed that changing the strength of the roof and floor surrounding rock and the cementation between coal pillars and surrounding rock can improve the bearing capacity of coal pillars under cyclic mining stress disturbance.

Previous studies on the cyclic loading of rocks have only focused on individual loading-unloading modes, and few have considered the influence of various loading-unloading modes on the mechanical properties of rocks. Therefore, this paper conducts cyclic loading-unloading experiments on sandstone by studying different loading-unloading modes, aiming to analyze the effects of loading-unloading on the mechanical parameters and energy evolution characteristics of sandstone.

2. Organization of the Text

2.1. Section Headings

In accordance with the standards of the International Society for Rock Mechanics (ISRM), standard cylindrical specimens with a dimension of φ50 mm × 100 mm were adopted, as illustrated in Figure 1 (with the allowable error of diameter and height not exceeding 2 mm). The wave velocity and density of the white sandstone were measured to be 2.4825 km/s and 2417.76 kg/m^3, respectively.

Figure 1. Sandstone Specimen

ISSN: 2710-0588

2.2. Test Equipment and Plan

The cyclic loading-unloading tests on sandstone were conducted using the RMT-150B rock mechanics test system, which was developed by Jinan Mine Rock Testing Instrument Co., Ltd. (as illustrated in Figure2).

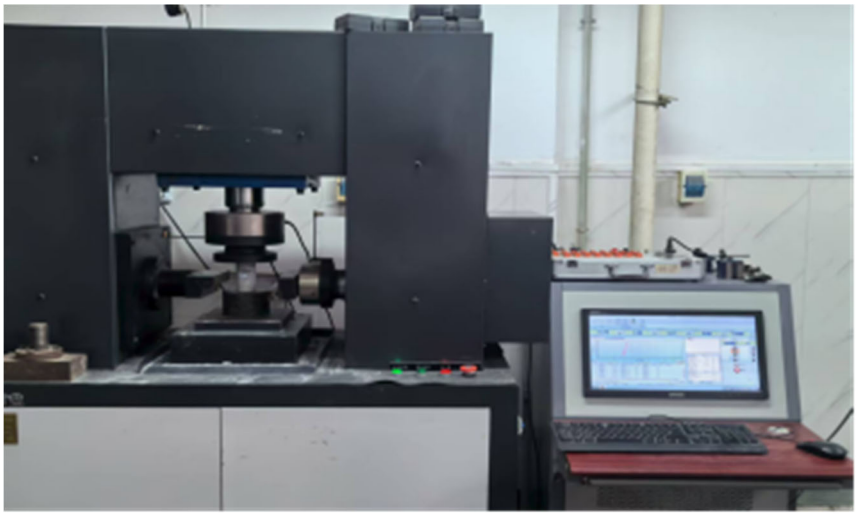

Figure 2. Experimental Equipment

The test scheme consists of three stages: specimen installation, uniaxial compressive test, and cyclic loading-unloading test, with the specific procedures as follows:

(1) Specimen installation: To minimize the phenomenon of hysteresis curve distortion caused by stress concentration due to eccentric loading during compression, firstly install both ends of the specimen into the chuck of the testing machine. Fine-tune the chuck position to align the specimen axis with the loading axis, which can be verified by the force sensor reading under no-load condition: if the no-load force is ≤ 0.5% of the full scale, the alignment is deemed qualified. Simultaneously install strain gauges, which are preheated for 10 minutes before zeroing.

(2) Uniaxial compressive test: After the specimen is installed, start the testing machine and load at a rate of 0.1 MPa/s until the specimen fails. The uniaxial compressive strength (UCS, denoted as σc) of the sandstone is measured to be approximately 60 MPa.

(3) Cyclic loading-unloading test: Two loading-unloading modes were adopted in the tests (the force-time curves are illustrated in Figure 3). Figure 3a shows the cyclic loading-unloading with variable upper limits: both the loading and unloading rates are set to 0.05 MPa/s. Initially, load to 12 MPa and hold for 10 seconds, then unload to 6 MPa and hold for 10 seconds; thereafter, the upper limit is increased by 12 MPa for each subsequent cycle until the rock specimen is crushed. Figure 3b shows the cyclic loading-unloading with variable upper and lower limits: the testing machine loads at a rate of 0.1 MPa/s to 12 MPa and holds for 10 seconds, then unloads to 10 MPa and holds for 10 seconds; thereafter, the upper limit of each subsequent loading is increased by 20% of σc until the specimen fails.

ISSN: 2710-0588

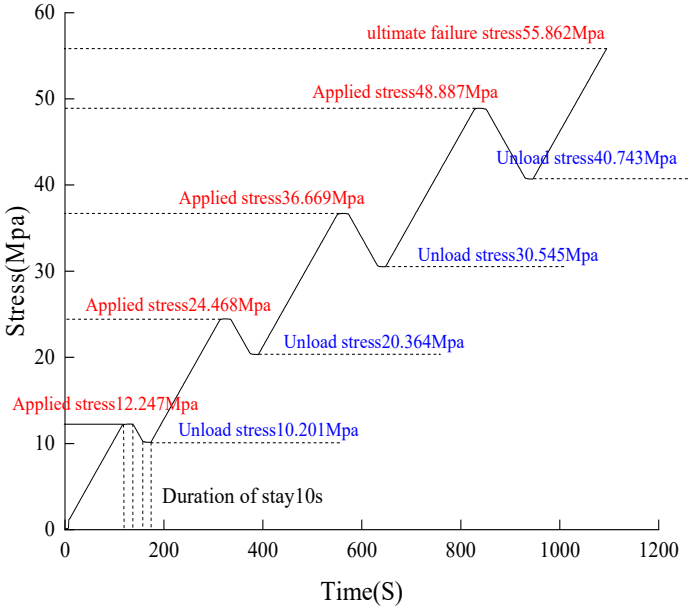

(a) Variable upper limit plus variable lower limit plus unloading method

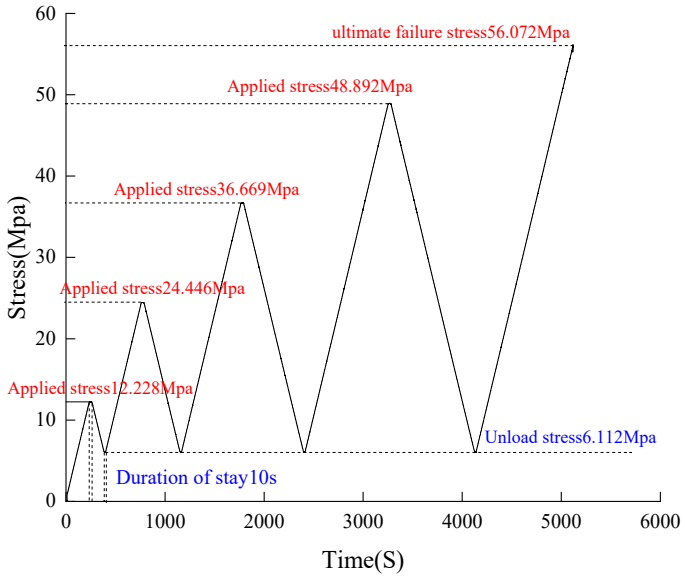

(b) Variable upper limit and unloading method

Figure 3. Stress Variation Over Time

3. Analysis of Test Results

3.1. Stress-strain curves for different loading and unloading methods

As can be seen from Figure 4, this loading mode characterized by fixed peak value and multi-stage cycles is designed to compare the cyclic response of the material under different stress levels, and to clarify the elastic limit, plastic yield point and damage degree of the material under various stress conditions. When the loading peak value is relatively low, the strain can be almost completely recovered after unloading, and the area of the hysteresis loop is small, indicating that the material is in the stage of elastic deformation. When the loading peak value exceeds a certain critical value, obvious residual plastic strain occurs after unloading, and the area of the hysteresis loop increases sharply, which demonstrates that the material enters the stage of plastic yielding. This critical value can be regarded as the yield strength or cyclic yield strength of the material [18]. The slopes (stiffness) of the loading-unloading curves

ISSN: 2710-0588

corresponding to different peak values exhibit discrepancies: the lower the peak value, the closer the stiffness is to the initial elastic stiffness; the higher the peak value, the more significant the stiffness degradation becomes due to the more severe plastic deformation and damage. Meanwhile, the hysteresis loop corresponding to a higher peak value has a larger area, which indicates that a higher stress peak value leads to a stronger energy dissipation capacity of the material, with more energy consumed by plastic deformation and damage.

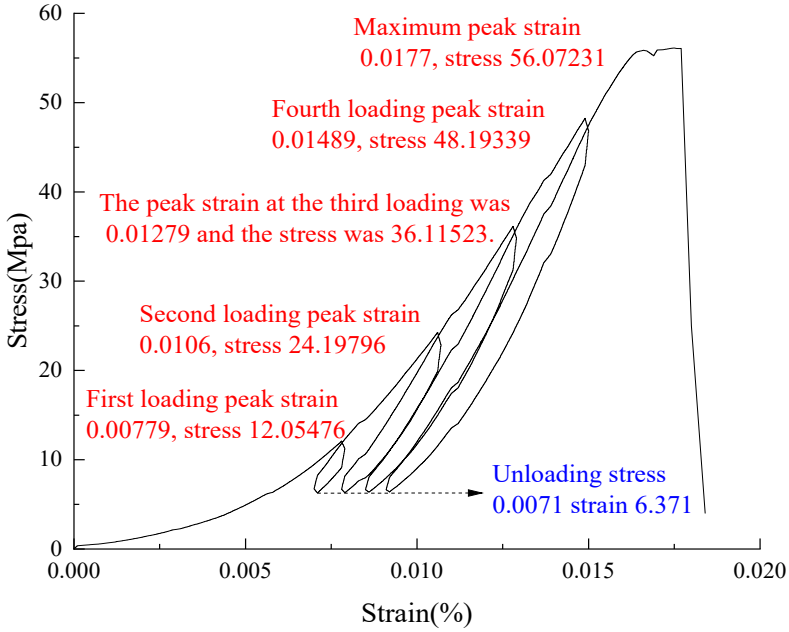

Figure 4. Load-Unload Stress-Strain Curve with Increased Upper Limit

As illustrated in Figure 5, this "increasing loading-unloading" mode (with both peak and valley values progressively increasing) simulates the material's response in a gradually intensifying cyclic stress field. Each cycle involves loading to a higher peak and unloading to a higher valley, reflecting the cyclic deformation behavior of the material as the stress level continuously elevates.

Loading phase: When the stress rises, the curve initially exhibits nonlinearity (indicating the material enters the elastoplastic stage) and subsequently tends to linearity (dominated by elasticity).

Unloading phase: "Stress hysteresis" occurs during stress reduction, demonstrating the generation of irreversible plastic deformation in the material. With an increase in the number of cycles and the elevation of peak stress, the cumulative effect of plastic deformation gradually becomes pronounced.

After multiple loading-unloading cycles, the slope of the loading phase (characterizing tangent stiffness) undergoes gradual changes, reflecting the accumulation of micro-damage induced by plastic deformation within the material, which leads to stiffness degradation. Meanwhile, the area of the hysteresis loop during unloading-reloading gradually expands, indicating that the material's energy dissipation capacity enhances with the increase in stress level. Damage induces internal friction or microcrack propagation, resulting in greater energy consumption.

ISSN: 2710-0588

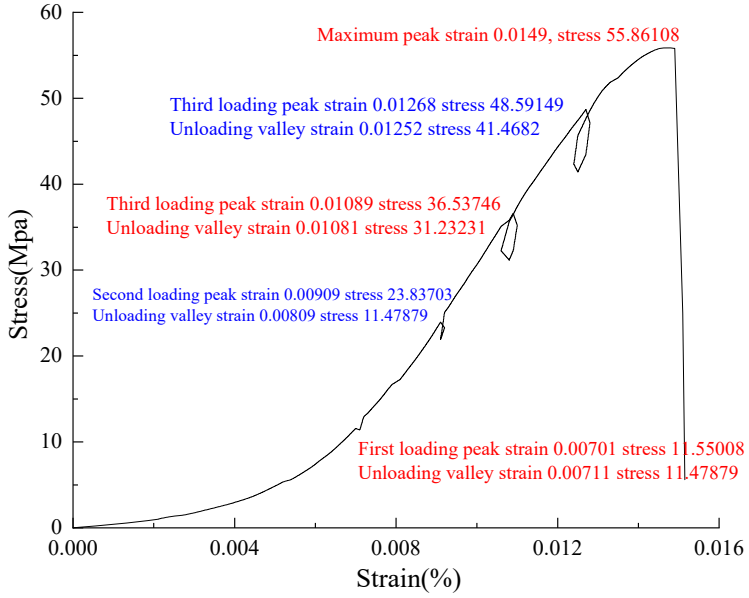

Figure 5. Stress-strain curve for variable upper limit, variable lower limit, and unloading

The comparison between the two different cyclic modes is intended to obtain the mechanical properties of rock specimens under distinct engineering scenarios. Mode 1 is designed to compare the elastic and plastic responses under different stress peak values, which is applicable for determining the elastic limit, yield strength and reliability of the material under various load conditions. Mode 2 focuses on the performance evolution of the material under progressively increasing cyclic stress, which is suitable for analyzing the fatigue damage of structures when subjected to gradually increasing loads.

3.2. Energy Calculation Method

The failure of rock is essentially a thermodynamic process, which involves the dynamic exchange of energy transfer and conversion between the rock and its external environment. Under cyclic loading, the total energy input into the rock is defined as the total input energy per unit volume. One portion of this energy is stored within the rock in the form of elastic strain energy, while the other portion is irreversibly dissipated as thermal energy, radiant energy, and other forms—this portion is referred to as the dissipated energy per unit volume [19].

To calculate the total input energy per unit volume, dissipated energy per unit volume, and elastic energy of sandstone specimens under cyclic loading-unloading, it is necessary to combine the geometric characteristics of the hysteresis loop under the stress-strain curve, following the subsequent steps and formulas:

The total input energy per unit volume corresponds to the total area under the stress-strain curve during the loading phase (i.e., the total energy input by external forces in a single cycle):

$$U_{\text{total}} = \int_0^{\varepsilon_{\max}} \sigma(\varepsilon) d\varepsilon$$

Where:σ= stress, ε= strain (integral variable)

The elastic energy per unit volume refers to the recoverable energy stored by elastic deformation during the unloading phase, which corresponds to the area under the unloading curve.

$$U_e = \frac{1}{2}\sigma_{\max} \bullet \varepsilon_e \quad or \quad U_e = \frac{\sigma^2_{\max}}{2E}$$

ISSN: 2710-0588

Where:σmax= maximum stress， E= elastic modulus

The dissipated energy per unit volume is represented by the area of the hysteresis loop (i.e., the irrecoverable energy).

$$U_d = \oint_{hysteresis\ loop} \sigma(\varepsilon) d\varepsilon$$

The total energy input into the rock by external forces is denoted as U. According to the First Law of Thermodynamics:

$$U_{total} = U_e + U_d ,$$

Where: The corresponding relationship between Ud and Ue is illustrated in the figure.

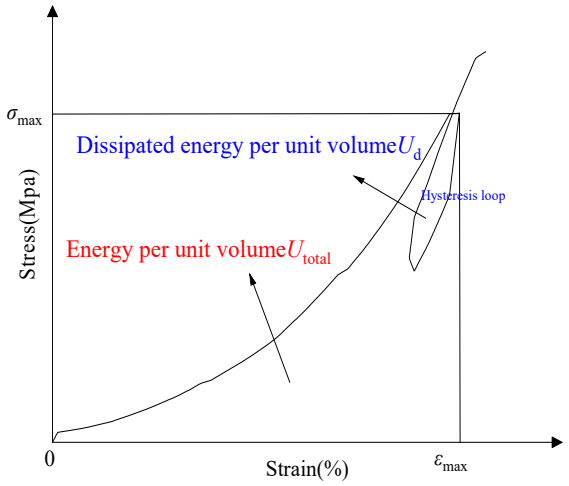

Figure 6. Relationship between unit volume elastic energy and unit volume dissipated energy

3.3. Energy evolution characteristics of different charging and discharging methods

The relationship between various energy parameters and the number of cycles during the cyclic process can be derived from the experimental data.

The total input energy per unit volume refers to the total energy input into the rock per unit volume by external forces during cyclic loading, and its evolution law is directly illustrated in Figure 7.

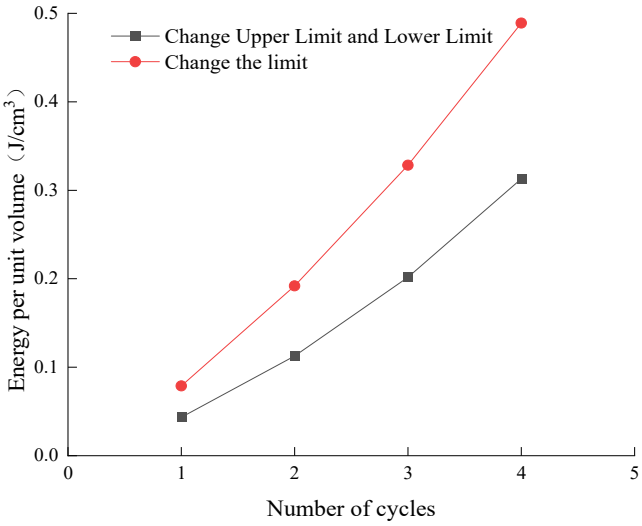

Figure 7. Variation of Unit Volume Energy with Number of Cycles

ISSN: 2710-0588

Cycle 1: Stage of Differential Response of Primary Fractures

Energy Dissipation Pathways

Variable upper limit mode: Intergranular fractures and microvoids inside the rock respond rapidly under peak load: a large number of primary fractures initiate, and some initiated fractures propagate over short distances; only a small amount of energy is allocated to elastic deformation, while most energy is concentrated on the initiation-preliminary propagation of primary fractures, resulting in relatively high energy consumption.

Variable upper and lower limit mode: The pre-compression effect of the initial lower limit forces some primary fractures into a state of micro-closure in advance. Peak load only induces the initiation of a small number of primary fractures without obvious propagation; most energy is used for elastic deformation, with only a small portion consumed in fracture initiation, leading to significantly lower energy consumption.

Cycle 2: Stage of Asymmetric Energy Consumption for Fracture Compaction

Energy Dissipation Pathways

Variable upper limit mode: Energy consumption is divided into two parts: (1) Compaction friction of semi-open fractures, dominated by the interlocking effect of rough protrusions on fracture surfaces; (2) Initiation and propagation of unresponsive primary fractures, where newly initiated fractures initially connect with pre-propagated ones. Only a small amount of energy is used for elastic deformation. The superposition of these two energy dissipation components leads to a significant increase in energy consumption during this stage.

Variable upper and lower limit mode: Energy consumption is dominated by compaction of closed fractures. The elevated lower limit enhances the contact tightness of fracture surfaces, and the compaction process needs to overcome stronger cohesive forces; only a small amount of energy is allocated to the initiation of unresponsive primary fractures, with another small portion consumed in elastic deformation. Due to the small increase in peak strain during this stage, no obvious fracture propagation occurs, resulting in only a slight rise in energy consumption.

Cycles 2–4: Stage of Rate Differentiation for Damage Accumulation

Energy Dissipation Pathways

Variable upper limit mode (Rapid damage accumulation): Energy dissipation pathways continue to expand. A portion of energy is used for the secondary propagation of interconnected fractures, where the fracture network evolves from linear branches to reticulated interweaving, and propagation needs to overcome friction across multiple fracture surfaces; another portion is consumed in the initiation of new fractures; the remaining part is allocated to sliding friction on fracture surfaces. Only a small amount of energy contributes to elastic deformation. Owing to the nonlinear connectivity of the fracture network, the energy consumption increment per cycle continuously increases, reflecting the characteristic of accelerated damage accumulation.

Variable upper and lower limit mode (Slow damage accumulation): Energy consumption is dominated by secondary opening of compacted fractures + initiation of a small number of new fractures. A portion of energy is used to overcome the resistance of secondary opening; since the elevated lower limit enhances the cohesive force of fracture surfaces, secondary opening requires overcoming higher resistance; another portion is consumed in the initiation of new fractures, where the small peak increment only activates near-surface micro-defects; the remaining part is allocated to elastic deformation. Restricted by limited fracture propagation, the energy consumption increment per cycle remains relatively stable, and damage accumulation exhibits the characteristic of gradual accumulation.

Cumulative Effect

ISSN: 2710-0588

The difference in damage accumulation between the two loading modes becomes increasingly pronounced with the increase of cycle numbers, leading to distinct differentiation in fracture network evolution and energy dissipation characteristics under different loading paths:

For variable upper limit loading: The fracture network gradually develops into a reticulated interwoven structure with cycling. The energy dissipation pathways during deformation also expand accordingly, including sliding friction across multiple fracture surfaces as well as the initiation and propagation of new fractures. This causes the growth rate of energy per unit volume to accelerate progressively, which exactly verifies the characteristic of nonlinear damage accumulation in rocks: the energy consumption required for the late-stage damage process exceeds that of the initial primary fracture initiation stage.

For variable upper and lower limit loading: The complexity of the fracture network is much lower than that in the variable upper limit scenario. The number of newly initiated fractures is small, and they only connect with a limited number of existing fractures. The expansion of energy dissipation pathways is relatively moderate, so the growth rate of energy per unit volume remains stable throughout the process. Although energy consumption also increases gradually in the late stage, the driving intensity for fracture propagation is weak, so the energy consumption value does not rapidly exceed the initial value of Cycle 1, unlike the variable upper limit mode.

The elastic energy per unit volume refers to the recoverable elastic strain energy of rocks during the unloading process, and its evolution law is illustrated in Figure 8.

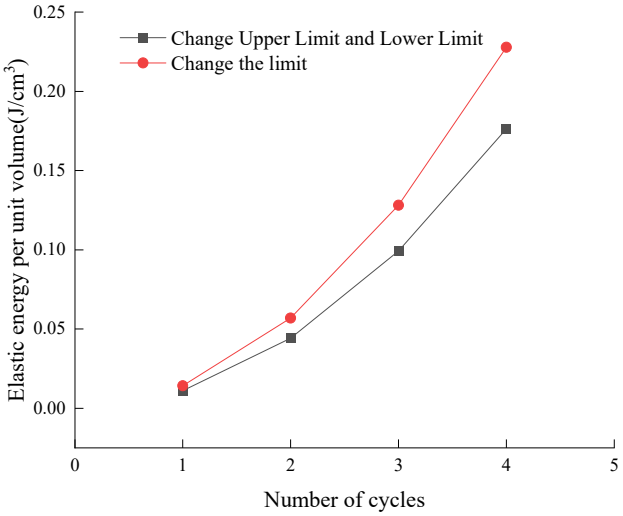

Figure 8. Variation of Elastic Energy per Unit Volume with Number of Cycles

Under both loading modes, the elastic energy accumulates continuously with increasing cycle numbers. The fundamental mechanism underlying this trend lies in the gradual densification and stabilization of the "elastic bearing system" within the rock during cyclic loading: as rock particles and fracture surfaces are subjected to repeated stress, initially loose gaps are compacted, forming a more stable elastic framework capable of sustaining external loads.

Differences in the stress application modes of the two loading methods lead to distinct rates of densification for the elastic bearing framework:

For the variable upper limit mode, the unidirectional increment of stress peaks directs the load specifically toward particle contact interfaces and fracture structures inside the rock. This results in a more targeted densification and interlocking process of the elastic bearing framework, accelerating the rate of structural stabilization and thereby significantly increasing the growth slope of elastic energy.

ISSN: 2710-0588

For the variable upper and lower limit mode, the simultaneous adjustment of upper and lower stress thresholds leads to bidirectional fluctuations in the stress application range. The compaction effect of the load on the elastic framework is distributed across a wider stress interval, resulting in a relatively gentle structural densification process and a correspondingly moderate growth rate of elastic energy.

From the perspective of the evolutionary mechanism of elastic energy: the test adopts a loading scheme with increasing maximum strain, which not only drives the synchronous rise of cyclic peak stresses but also enhances the bearing stiffness (elastic modulus) of the elastic bearing framework through the compaction effect of cyclic loading. The synergistic coupling of these two factors gives rise to the cumulative growth of elastic energy with a continuously accelerating rate.

This trend also reflects an increase in the proportion of reversible deformation of the rock under cyclic loading: the higher the stability of the elastic bearing framework, the greater the proportion of recoverable elastic deformation under external forces. The continuous growth of elastic energy is a direct manifestation of the gradual stabilization of the internal rock structure, while the stress application mode of different loading methods determines the rate difference in this structural stabilization process.

The dissipated energy per unit volume refers to the irrecoverable energy during the cyclic process (e.g., fracture propagation work, particle friction heat, etc.). Its evolution law, illustrated in Figure 9, can be clearly divided into three stages:

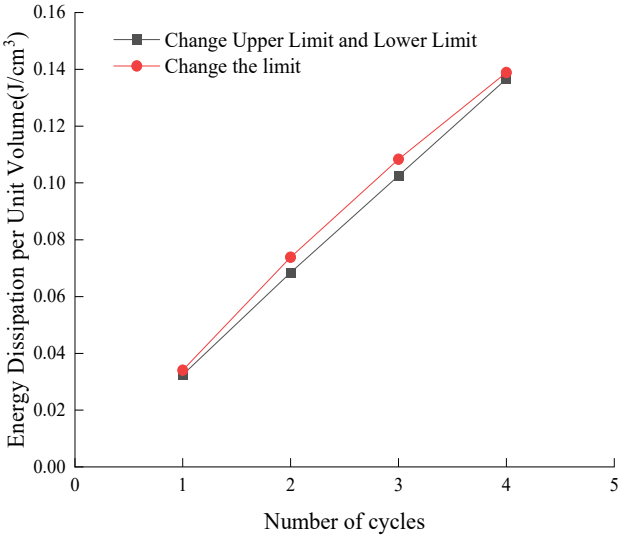

Figure 9. Variation of unit volume dissipated energy with the number of cycles

Stage 1: Cycle 1→2 — Initial Rise Period of Dissipated Energy

During the first to second cycles, the dissipated energy increases slightly from approximately 0.04 J/cm^3 to 0.05–0.06 J/cm^3. The dominant mechanism of energy dissipation in this stage is the preliminary initiation of primary fractures and interface running-in. In the first cycle, a small number of primary micro-fractures inside the rock initiate under stress; however, since the applied strain remains in the initial range, the extent of fracture propagation is limited, and energy dissipation is dominated by preliminary friction on fracture surfaces. In the second cycle, the slight increment of applied strain induces the initiation of more primary fractures, accompanied by further frictional sliding on the surfaces of already initiated fractures. The combined effect of these two processes drives a modest increase in dissipated energy. This stage represents the incubation period of initial rock damage, characterized by a low degree of damage.

ISSN: 2710-0588

Stage 2: Cycle 2→3 — Rapid Rise Period of Dissipated Energy

From the second to third cycles, the dissipated energy surges from 0.05–0.06 J/cm^3 to approximately 0.10 J/cm^3, with a markedly expanded growth amplitude. The energy dissipation mechanism in this stage shifts to fracture propagation and preliminary network construction. After the first two cycles, the primary fracture system has been partially activated; under the increasing strain loading, fractures break through the initial propagation threshold, extending in depth and achieving preliminary connection. Meanwhile, the multi-interface friction and dislocation effects within the fracture network are intensified, leading to an increase in energy dissipation pathways and thus accelerating the growth rate of dissipated energy. This stage signifies the entry of rock damage into the rapid development period.

Stage 3: Cycle 3→4 — Accelerated Rise Period of Dissipated Energy

During the third to fourth cycles, the dissipated energy experiences a substantial surge: rising to approximately 0.16 J/cm^3 under the variable upper limit mode and to around 0.14 J/cm^3 under the variable upper and lower limit mode, representing the most significant growth amplitude across all stages.

The core energy dissipation mechanism in this stage lies in the through-going propagation of the fracture network and the differentiation of stress effects induced by different loading modes. After the first three cycles, an interwoven fracture network has formed inside the rock; the increasing strain loading in the fourth cycle pushes the peak stress beyond the critical threshold for coordinated propagation and connection of fractures. Fractures then transition from dispersed propagation to synchronous extension and connection of multiple fractures. This process requires overcoming the spatial constraints and interfacial cohesive forces of the fracture network, resulting in a significant increase in both the total amount and rate of energy dissipation.

The differences between the two loading modes become more pronounced in this stage. The variable upper limit mode adopts a unidirectional increment pattern of stress peaks, where stress acts intensively on the extending tips of the fracture network, facilitating rapid through-going of fractures and thus yielding a steeper growth slope of dissipated energy. In contrast, the variable upper and lower limit mode features bidirectional fluctuations in the stress range; although it enhances the repeated frictional dissipation on fracture surfaces, the increment amplitude of peak stress is smaller than that of the variable upper limit mode. Consequently, the total dissipated energy is slightly lower while still maintaining a high growth rate. This stage marks the rock's entry into the critical development period of fatigue damage, where the fracture network approaches the critical state of macroscopic connection.

The evolution of total input energy per unit volume, elastic energy, and dissipated energy is not isolated but exhibits a tight coupling relationship. Combining the variation characteristics of energy parameters in the figures, the evolutionary trajectory of total input energy is essentially the integrated effect of elastic energy growth and the stage-wise rise of dissipated energy:

In Cycle 1, the total input energy remains in the initial low range. This is rooted in the relatively limited proportion of elastic energy and the dominance of dissipated energy as the primary energy dissipation pathway, with both energy components staying at the initial evolutionary level.

During Cycle 1→2, the total input energy shows a slight upward trend, which is the superimposed effect of the initial growth of elastic energy and the modest rise of dissipated energy, with the proportions of the two energy components remaining relatively balanced.

In Cycle 2→4, the total input energy enters a period of substantial and continuous growth. The core driving mechanism is the synergistic rise of elastic energy and dissipated energy, coupled with the amplification effect of increasing strain loading on the energy input scale, leading to a gradual expansion of the growth amplitude of total input energy.

ISSN: 2710-0588

Among these, the continuous growth of elastic energy is a direct manifestation of the densification of the rock's elastic bearing framework and the enhancement of its load-bearing capacity. Meanwhile, the stage-wise rise of dissipated energy (from gentle growth to substantial increase) in the figures serves as an intuitive measure of rock damage evolution from initiation and propagation to network connection. Together, they construct a complete energy chain of deformation energy storage-damage energy dissipation-structural instability for rocks under cyclic loading.

Therefore, despite the adoption of different loading-unloading modes, these modes are designed to demonstrate the mechanical properties exhibited by rocks under distinct load conditions.

3.4. Derived Energy Parameters

3.4.1. Energy conversion efficiency

The calculation of energy conversion efficiency is centered on the proportional relationship between elastic energy and total input energy, which is defined by the following formula:

$$\eta = \frac{U_e}{U_{total}} \times 100\%$$

The essence of this calculation logic lies in quantifying the distribution relationship between the recoverable elastic component and the irrecoverable damage-related component within the total input energy via the "elastic energy ratio".

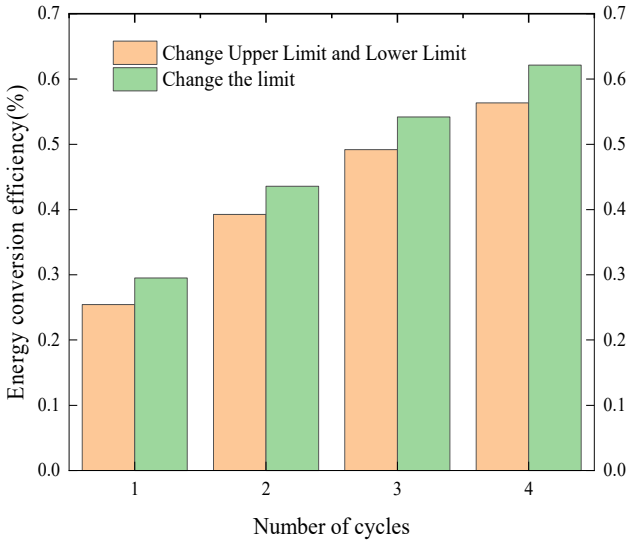

Figure 10. Energy Conversion Efficiency Diagram

As illustrated in Figure 10, both curves exhibit a continuous upward trend with increasing cycle numbers: rising gradually from the low range of 0.25–0.30 at Cycle 1.0 to the interval of 0.56–0.62 at Cycle 4.0. This trend intuitively reflects that with the progression of cyclic loading, the compaction and strengthening effect of the elastic bearing framework inside the rock becomes increasingly prominent, leading to a sustained increase in the proportion of elastic energy in the total input energy and a continuous enhancement of energy storage capacity.

From a physical perspective, energy conversion efficiency serves as a direct quantitative characterization of the "structural integrity of the elastic bearing system" within the rock:

A higher efficiency indicates a larger proportion of total input energy allocated to elastic energy storage, signifying a more stable elastic framework formed by cyclic compaction and a smaller proportion of energy consumed by damage processes.

ISSN: 2710-0588

Conversely, a lower efficiency implies that more total input energy is dissipated through irreversible damage processes such as fracture initiation and interface friction, indicating weaker structural integrity of the rock.

The efficiency comparison between the two loading-unloading modes further reveals the differential regulatory effect of stress application modes on energy distribution:

The efficiency of the variable upper limit mode is consistently higher than that of the variable upper and lower limit mode. This is attributed to the unidirectional increment of stress peaks in the variable upper limit mode, which focuses stress action on the compaction of the elastic bearing framework, weakening the additional damage energy consumption caused by scattered stress fluctuations and thus promoting a continuous increase in the proportion of elastic energy in the total input energy.

In contrast, the variable upper and lower limit mode adjusts both upper and lower stress thresholds simultaneously, and the bidirectional fluctuations in the stress range tend to increase damage energy consumption such as friction and relaxation on fracture surfaces. This results in a relatively lower proportion of elastic energy and correspondingly weaker efficiency.

The value of this indicator lies not only in quantitatively distinguishing the energy distribution mechanisms of different loading modes but also in serving as an "energy-based quantitative criterion" for rock damage evolution. Specifically, the continuous increase in efficiency corresponds to the gradual compaction and strengthening of the elastic bearing framework, while the efficiency gap between the two modes essentially reflects the regulatory effect of stress application modes on the proportion of damage energy consumption.

3.4.2. Rate of increase of dissipated energy density

The dissipated energy density growth rate λ_d is a core energy indicator for quantifying the acceleration degree of damage evolution in rock cyclic loading tests. It refers to the ratio (expressed as a percentage) of the difference in dissipated energy density between two adjacent cycles to the dissipated energy density of the previous cycle, and is used to characterize the variation in the growth rate of damage-induced energy dissipation. It is defined by the following formula:

$$\lambda_d = \frac{U_{d,\,n} - U_{d,\,n-1}}{U_{d,\,n-1}} \times 100\%$$

The calculation results are presented in the following table:

Table 1. Calculation Table of Dissipated Energy Density Growth Rate

Number of cycles	Dissipated energy per unit volume (J/cm³)		Rate of increase of dissipated energy density	
	Change Upper Limit and Lower Limit	Change the limit	Change Upper Limit and Lower Limit	Change the limit
1	0.0324	0.0341		
2	0.0684	0.0738	1.1099	1.168
3	0.1025	0.1084	0.4986	0.4678
4	0.1366	0.1389	0.3326	0.2816

Stage of High Growth Rate (Cycle 1→2): Corresponding to the Initial Damage Burst Period

Primary micro-fractures inside the rock initiate and propagate intensively under the stress of the first cycle, which requires overcoming the particle cementation force and fracture surface energy. This causes the dissipated energy to rise rapidly from an extremely low base value, and

ISSN: 2710-0588

the growth rate exhibits a burst-type peak, reflecting the characteristic of concentrated initiation of damage.

Stage of Declining Growth Rate (Cycle 2→3): Corresponding to the Damage Transition Period

Primary fractures are almost fully activated, and the damage mechanism shifts to frictional sliding of residual fractures and propagation of a small number of newly generated micro-fractures. The scale of energy dissipation narrows significantly, and the growth rate drops rapidly, indicating that the acceleration degree of damage begins to decay.

Stage of Stable Growth Rate (Cycle 3→4): Corresponding to the Steady Development Period of Fatigue Damage

After multiple cycles of compaction, the load-bearing capacity of the elastic framework is enhanced, and the growth rhythm of energy dissipation induced by newly generated damage (fracture propagation and friction) tends to stabilize. The growth rate decreases continuously and approaches a steady state, reflecting the evolution of damage from disordered and intense to ordered and cumulative.

The variation trend of the dissipated energy density growth rate clearly reveals that rock fatigue damage does not develop at a constant speed; instead, it exhibits a non-uniform characteristic of being fast initially and then slowing down to gradually stabilize. This law breaks the simplistic assumption that damage increases linearly with the number of cycles, and provides a quantitative basis for the accurate division of rock damage stages under cyclic loading.

3.5. Derived Energy Parameters

Difference Analysis Based on Macroscopic Failure Characteristics of Specimens Under Two Loading-Unloading Modes (Figure 11)

1. Differences in Fracture Morphology Characteristics

For the variable upper limit cyclic loading-unloading condition: The specimen exhibits a splitting failure mode dominated by a single vertical main crack. The fracture develops along the maximum principal stress direction (vertical), characterized by a small number of fractures with significant penetrability. Obvious cracking features only appear in the main crack zone, while the specimen maintains an overall cylindrical geometric shape without large-scale disintegration [20].

For the variable upper and lower limit cyclic loading-unloading condition: The specimen shows a diffuse failure mode controlled by a multi-directional fracture network. The fracture system includes vertical, inclined, and other directions, with non-directionality in micro-fracture initiation and propagation, forming a complex spatial fracture network. The failure process is not dominated by a single main crack, and the synergistic evolution characteristics of multi-zone cracking are observable on the specimen surface.

2. Differences in Damage Accumulation and Evolution Mechanisms

Variable upper limit mode: Damage evolution follows a directional superposition effect. The stress path presents a monotonically increasing cyclic pattern; each increase in loading peak only drives the propagation of the main crack along the maximum principal stress direction. Residual deformation during unloading is concentrated in the main crack zone, and damage accumulates gradually through directional superposition, ultimately resulting in the penetration failure of a single main crack.

Variable upper and lower limit mode: Damage evolution exhibits a multi-scale propagation effect. The bidirectional variation of the stress path induces the initiation and propagation of micro-fractures in different stress intervals, leading to multi-scale and decentralized damage accumulation inside the specimen. During the loading-unloading cycles, multi-zone damage

ISSN: 2710-0588

evolves synergistically, and the final failure is characterized by the synergistic penetration of a multi-fracture network.

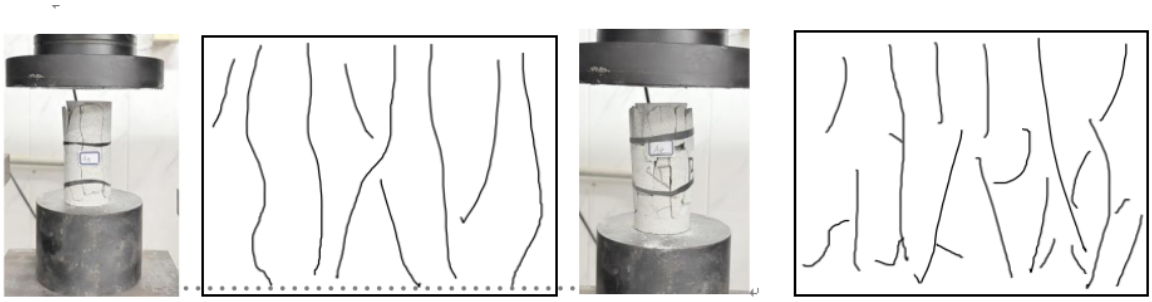

Figure 11. Macroscopic Damage Features and Fracture

It can be concluded from the macroscopic failure characteristics that the differences in loading-unloading modes and the durations of the entire processes give rise to the variations in the final failure patterns of the specimens.

4. Conclusion

Based on the above experimental data, the following conclusions are drawn:

Both the variation of stress peaks and cyclic loading-unloading exert significant influences on the mechanical and energy characteristics of the material. At different stress peaks, the stiffness of the loading-unloading curve degrades more significantly with the increase of peak stress, which is attributed to the aggravation of plastic deformation and internal damage. Meanwhile, a higher stress peak corresponds to a larger hysteresis loop area, indicating a stronger energy dissipation capacity of the rock. After multiple cyclic loading-unloading processes, the gradual change in the slope of the loading segment reflects the stiffness degradation induced by the accumulation of micro-damage. The progressive increase in the area of the hysteresis loop during unloading and reloading demonstrates that the elevated stress level enhances the energy dissipation capacity, where the internal friction and micro-fracture propagation caused by damage consume more energy.

The differences in energy evolution between the two loading modes are entirely determined by the stress application patterns. The stress concentration effect of the variable upper limit mode not only accelerates the compaction of the elastic bearing framework but also induces more damage-related energy dissipation. Consequently, the growth amplitudes of total input energy, elastic energy, and dissipated energy under this mode are significantly higher than those under the variable upper and lower limit mode. In contrast, the latter mode weakens stress concentration by synchronously adjusting the upper and lower stress limits, resulting in a relatively gentle growth rhythm of all energy parameters.

The energy conversion efficiency increases continuously with the number of cycles, which reflects the compaction and strengthening of the rock's elastic bearing framework and the improvement of its energy storage capacity. The variable upper limit mode yields higher energy conversion efficiency due to its stress concentration effect that facilitates elastic energy storage, whereas the variable upper and lower limit mode suffers from additional damage energy consumption caused by stress fluctuations, leading to lower efficiency.

The dissipated energy density growth rate is a core indicator for quantifying the acceleration degree of rock damage evolution. The data show that it exhibits a trend of bursting-declining-stabilizing, which corresponds to the three stages of initial damage burst, damage transition,

ISSN: 2710-0588

and steady damage development. This trend reveals the non-uniform characteristic of rock damage evolution, i.e., developing rapidly at the initial stage and then slowing down gradually.

Under the variable upper limit cyclic loading-unloading condition, the specimen undergoes splitting failure dominated by a single vertical main crack. Its damage evolution follows the directional superposition effect: the main crack propagates directionally along the maximum principal stress direction, and the residual deformation is concentrated in the main crack zone. In contrast, under the variable upper and lower limit cyclic loading-unloading condition, the damage evolution of the specimen exhibits the multi-scale propagation effect: micro-fractures in multiple stress intervals initiate and propagate synergistically, and multi-zone damage accumulates synchronously, ultimately resulting in the synergistic penetration of a multi-fracture network.

References

[1] Lin, Z. N., Long, H. F., & Zhang, Q. (et al.). Experimental study on the permeability characteristics of sandstone under different temperature and confining pressure cycling loading and unloading. *Journal of Hydraulic and Maritime Engineering*, 1–15. [2025-09-13]. (Online advance publication).

[2] Zhu, M. L., Ma, Y. S., & Qin, G. P. (et al.). Mechanical characteristics and stability analysis of surrounding rock in shallow buried tunnels under cyclic loading and unloading. *China Mining*, 34(S1), 360–366.

[3] Ni, Z., Li, J., & Qin, K. (et al.). Experimental study on the mechanical properties and deformation failure characteristics of sandstone under graded equal-amplitude cyclic loading and unloading. *Scientific Reports*, 15(1), 28735. https://doi.org/10.1038/s41598-025-04216-7

[4] Liu, Y. M., Li, Z., & Feng, G. R. (et al.). Characteristics and precursor patterns of acoustic-thermal responses in fractured sandstone under cyclic loading-unloading. *Geotechnical Mechanics*, 46(9), 2773–2791.

[5] Yang, H., Song, Y., & Ren, J. (et al.). Study of the evolution of characteristic parameters and damage mechanism of sandstone under the synergistic effects of F-T and stepped cyclic loading-unloading via real-time CT scanning and AE monitoring. *Measurement*, 256, 118078. https://doi.org/10.1016/j.measurement.2025.118078

[6] Song, Y. Z., Zhang, H. W., & Yu, Z. (et al.). Mechanical responses of sandstone exposed to triaxial differential cyclic loading with distinct unloading rates of confining stress: A lab scale investigation. *International Journal of Coal Science & Technology*, 12(1), 58. https://doi.org/10.1007/s40789-024-00689-2

[7] Zhang, Q. H., Meng, X. R., & Zhao, G. M. (2025). Energy evolution laws of sandstone under different cyclic loading and unloading modes of true triaxial stress. *Journal of Mining Science*, 10(3), 418–434.

[8] Zhu, N. Q., Li, X. L., & Chen, S. J. (et al.). Deformation failure and acoustic emission response characteristics of fractured sandstone under cyclic loading and unloading. *Coal Science and Technology*, 1–19. [2025-09-13]. (Online advance publication)

[9] Hao, J. P., Dong, C. L., & Yao, M. Y. (2025). Study on the damage mechanics characteristics and energy evolution of hard rock under different upper limit stress cyclic loading and unloading. *Mining Research and Development*, 45(3), 119–127.

[10] Cheng, J. C., Liu, Y. T., & Zhang, L. (et al.). Mechanical abrupt behavior of sandstone under triaxial cyclic loading and unloading after peak. *Journal of Rock Mechanics and Engineering*, 44(4), 850–864.

[11] Tang, J. Z., Tang, W. H., & Yang, K. (et al.). Mechanical response characteristics and seepage evolution laws of inclined single-fracture sandstone under cyclic loading. *Rock and Soil Mechanics*, 46(1), 199–212.

[12] Xiao, F. K., Mo, R. H., & Shan, L. (et al.). Study on the damage characteristics of multi-stage characteristic stress cyclic loading and unloading in rocks. *Journal of Mining and Safety Engineering*, 42(2), 430–439.

ISSN: 2710-0588

[13] Wang, M. X., Wang, H., & Ma, S. L. (et al.). Energy dissipation experimental study of explosion-damaged roof sandstone under triaxial graded cyclic loading and unloading. *Vibration and Shock*, 43(16), 227–237.

[14] Cheng, J. C., Jia, Z., Hou, M. D., et al. (2024). Analysis of deformation characteristics of sandstone under triaxial cyclic loading and unloading and study on expanded infiltration model. *Journal of Rock Mechanics and Engineering*, 43(11), 2687–2699.

[15] Liu, G. J., Zhou, H., Mou, Z. L., et al. (2025). Research on macro-micro damage characteristics of fractured sandstone under variable upper limit cyclic loading and unloading. *Coal Science and Technology*, 53(5), 77–89.

[16] Jia, P., Wang, Y., Wang, Q. W., et al. (2024). Experimental study on the resistivity and acoustic emission response of red sandstone under cyclic loading and unloading conditions. *Journal of Rock Mechanics and Engineering*, 43(S1), 3333–3341.

[17] Zhao, G. Z., Cheng, W., Liu, C., et al. (2024). Study on the damage mechanical behavior and energy evolution of coal rock mass based on cyclic loading and unloading. *Journal of Rock Mechanics and Engineering*, 43(7), 1636–1645.

[18] Yuan, H. C., Abir, Zhang, J., et al. (2023). Experimental study on the deformation and failure characteristics of saturated fine yellow sandstone under graded cyclic loading and unloading. *Journal of Rock Mechanics and Engineering*, 42(S2), 3943–3955.

[19] Song, Y. M. (2025). Study on energy evolution and failure characteristics of sandstone under cyclic loading/unloading. *Journal of Safety Science*, 35(S1), 158–165.

[20] Li, X. W., Yao, Z. S., Huang, X. W., et al. (2021). Study on deformation damage characteristics and energy evolution of sandstone under cyclic loading and unloading. *Rock and Soil Mechanics*, 42(6), 1693–1704.